Drifting cavity solitons and dissipative rogue waves induced by time-delayed feedback in Kerr optical frequency comb and in all fiber cavities

Mustapha Tlidi,[1] Krassimir Panajotov,[2] Michel Ferré,[3] and Marcel G. Clerc[3]
[1]*Faculté des Sciences, Optique Nonlinéaire Théorique, Université libre de Bruxelles (U.L.B.), C.P. 231, Campus Plaine, B-1050 Bruxelles, Belgium*
[2]*Department of Applied Physics and Photonics (IR-TONA), Vrije Universiteit Brussels, Pleinlaan 2, B-1050 Brussels, Belgium*
[3]*Departamento de Física, FCFM, Universidad de Chile, Casilla 487-3, Santiago, Chile*

(Received 14 May 2017; accepted 5 September 2017; published online 19 October 2017)

Time-delayed feedback plays an important role in the dynamics of spatially extended systems. In this contribution, we consider the generic Lugiato-Lefever model with delay feedback that describes Kerr optical frequency comb in all fiber cavities. We show that the delay feedback strongly impacts the spatiotemporal dynamical behavior resulting from modulational instability by (i) reducing the threshold associated with modulational instability and by (ii) decreasing the critical frequency at the onset of this instability. We show that for moderate input intensities it is possible to generate drifting cavity solitons with an asymmetric radiation emitted from the soliton tails. Finally, we characterize the formation of rogue waves induced by the delay feedback. *Published by AIP Publishing.* https://doi.org/10.1063/1.5007868

The formation of temporal cavity solitons (CS) and their relation to optical comb generation in a standard silica fiber cavity and in a continuous-wave (CW) driven nonlinear optical microresonator has been recently established both numerically and experimentally. Optical frequency combs are sources with a spectrum consisting of millions of equally spaced laser lines. This unique property provides a link between the optical and the radiofrequency band of the electromagnetic spectrum and it has truly revolutionized a number of research disciplines, such as precision laser spectroscopy and frequency metrology. In this paper, we show that delay feedback can control the mobility of cavity solitons leading to optical frequency comb generation, as well as the generation of rouge waves in driven cavities such as whispering-gallery-mode microresonators. In absence of delay feedback, it is usually hard to reach the rogue wave regime with a continuous wave injection beam. However, by using the time-delayed feedback we can reduce the threshold associated with modulational instability, self-pulsating cavity solitons and rogue waves generation.

I. INTRODUCTION

In 1987, Lugiato and Lefever (LL) derived a mean-field model often called the Lugiato and Lefever equation (LLE) that has been widely used to describe optical dissipative structures in cavity nonlinear optics.[1] Since then, this simple and universal model has been derived from various optical systems. The LLE constitutes a well-known paradigm for the study of dissipative structures that can be either periodic or localized in the transverse plane of the optical cavity. This pioneering work established the link between the transverse instability inherent in broad areas optical systems and the classical Turing–Prigogine instability well-known in reaction-diffusion chemical systems.[2–4] The wavelength of the spatially periodic pattern emerging from this instability is intrinsic to the dynamics which is solely determined by the dynamical parameters and not by the external effects or physical geometrical boundaries. The LLE has been derived for passive diffractive nonlinear cavities filled with liquid crystal operating in a self-imaging configuration,[5] left-handed materials,[6,7] and photonic coupled waveguides.[8] It has been also derived from dispersive systems such as a nonlinear fiber resonator[9] and whispering-gallery-mode microresonators leading to optical frequency comb generation.[10–15] The modeling of broad area resonators where diffraction and dispersion have comparative influence leads to the three-dimensional LLE in Ref. 16–19. Theoretical and experimental studies have been carried out on spatial and/or temporal confinement of light leading to the formation of cavity solitons (CS's). This is a well documented issue as can be seen from recent overviews.[20–29]

Here, we investigate the effect of time-delayed feedback control on the formation of temporal cavity solitons and rogue waves in the Lugiato–Lefever equation. Time delayed feedback describes how the state of the system at the current moment of time is affected by its value at some time in the past.[30] As a matter of fact, this feedback impacts strongly the space-time dynamics and affects both the modulational instability threshold and the period of the emerging train of pulses from this instability. It is well known that delay-induced motion of CSs has been predicted to manifest itself in the form of short optical pulses propagating in a cavity[31–33] and a laser[34,35] system. Recent studies on vertical cavity surface-emitting lasers (VCSELs) subjected to injection and to delay feedback[36–38] have shown that the phase of the delayed feedback and carrier decay rate strongly impact the parameter region where CSs become unstable and exhibit a spontaneous drift with a constant speed. These theoretical predictions

remain to be confirmed experimentally. The stability of a steady-state front subject to a time-delayed feedback control has been examined in Ref. 39. Time-delayed feedback control has also been investigated in the reaction-diffusion context.[40–43] Stability of plane wave solitons in the complex Ginzburg–Landau equation with delayed feedback has been investigated in Ref. 44.

In another line of research it has been shown that in small area optical cavities where the diffraction is neglected, the time-delayed feedback can generate temporal rogue waves.[45] Rogue waves are rare optical giant pulses or extreme events that occur in the supercontinuum generated by a photonic crystal.[46] Since this seminal work, optical rogue waves have been intensively investigated.[47–50] Rogue waves have been generated in whispering gallery mode resonators leading to frequency comb generation.[14] More recently, rogue waves have been predicted and experimentally observed in a semiconductor microcavity laser with an intracavity saturable absorber.[51,52]

In this paper, we analyze the formation of temporal cavity solitons, self-pulsating cavity solitons, and rogue waves in an all fiber cavity driven by a coherent injected beam with a time-delayed feedback loop. We show that the modeling of this simple device leads to the well known Lugiato–Lefever model with time-delayed feedback. We, therefore, provide the temporal analog of the spatial Kerr system cavity. We show that the delay feedback can induce drift instability leading to the motion of temporal cavity solitons with a constant speed. In the absence of time-delayed feedback control, temporal cavity solitons do not exhibit drift instability. We also show that the dispersive (Cherenkov) radiation emitted by a drifting cavity soliton is asymmetric. This is due to the broken reflection symmetry induced by the time-delayed feedback. Finally, we show that rogue wave formation can occur for moderate injected field intensities. This is quite important from a practical point of view as it facilitates the experimental observation of temporal dissipative rogue waves in continuous-wave driven nonlinear optical microresonators.

The paper is organized as follows, after an introduction, we derive in Sec. II, the Lugiato–Lefever equation with an additional term that accounts for the time delayed feedback. In Sec. III, we perform a linear stability analysis. Drifting cavity solitons and rogue wave generation by the delay feedback are discussed in Sec. IV. We conclude in Sec. V.

II. LUGIATO–LEFEVER MODEL WITH TIME-DELAYED FEEDBACK

Let us consider a nonlinear cavity filled with a Kerr medium and subjected to an external coherent beam. This cavity can be a fiber resonator or whispering-gallery disk microresonators and is schematically depicted in Fig. 1. It consists of a cavity of radius $r = L/2\pi$. The delayed feedback is introduced by an external loop with a large radius $r_{ext} = L_{ext}/2\pi$, as shown schematically in Fig. 1. The delay time $\tau = L_{ext}n_f/c$ corresponds to the light travel-time in the external loop with c being the speed of light and n_f - the refractive index of the fiber. A continuous wave of power E_{in}^2 is launched into the cavity by means of a beam splitter, propagates inside the fiber,

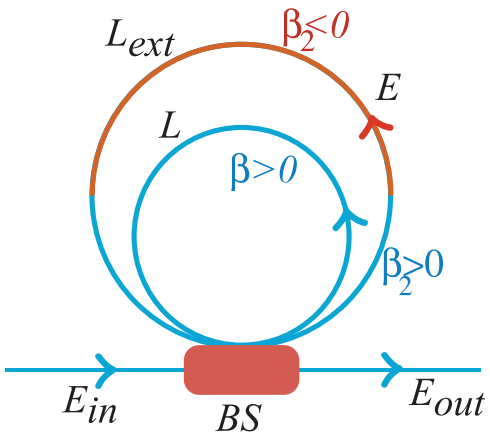

FIG. 1. Schematic representation of the setup of a ring nonlinear cavity with an external feedback delayed loop. E_{in} is the amplitude of the injected field and BS denotes the beam splitter.

and experiences dispersion and Kerr nonlinearity. In what follows, we assume that the dispersion in the external cavity is compensated by periodic group velocity dispersion management with zero average value. Indeed, we consider that a half of the external cavity has a normal dispersion ($\beta_2 < 0$) and the other operates in the anomalous dispersion regime ($\beta_2 > 0$). Light propagation in the cavity is ruled by the dimensionless nonlinear Schrödinger equation

$$\frac{\partial E}{\partial z} = i\beta\frac{\partial^2 E}{\partial \xi^2} + i|E|^2E, \tag{1}$$

where $E(z, \xi)$ is the slowly varying electric field envelope, z is the longitudinal coordinate along the optical axis, ξ is the time in a reference frame traveling at the group velocity of light in the Kerr material, and β is the dispersion coefficient inside the cavity which we assume to be positive, that is, corresponds to an anomalous dispersion. To simplify further the modeling of the system, we assume that the length of both loops is equal, i.e., $L = L_{ext}$. In this case, the delay time is fixed and we vary the strength of the delay feedback. At each round trip, the light inside the fiber is coherently superimposed with the input beam. This can be described by the boundary conditions that are compatible with all fiber cavities

$$\begin{aligned} E_{p+1}(z=0) &= TE_{in} + R\exp(-i\phi) \\ &E_p(z=L) + R'\exp(-i\phi')E_p(z=L,p), \end{aligned} \tag{2}$$

where $E_p(z)$ is the electric field envelope during the p^{th} pass in the internal cavity. The parameters R and T (R' and T') are, respectively, the reflection and transmission coefficients of the cavity (external cavity) beam-splitter.

By averaging of the right-hand side of Eq. (1) over one cavity length, we get

$$\begin{aligned} E_p(z=L) - E_p(z=0) &= iL\beta\frac{\partial^2 E_p(z=0)}{\partial \xi^2} \\ &+ iL|E_p(z=0)|^2E_p(z=0). \end{aligned} \tag{3}$$

The nonlinear Schrödinger equation supplemented by the cavity boundary conditions constitutes an infinite-dimensional

map. To simplify the theoretical analysis of the problem, it is convenient to reduce this map to a single partial differential equation. To do this, we restrict our analysis to high finesse cavities, i.e., $R \ll 1$ ($T \approx 1 - R^2/2$). In this case, the temporal evolution of the field inside the cavity is slow with respect to the round-trip time t_r. We can thus consider that this evolution is continuous and we can replace the map index p by a slow time scale t for the description of the field evolution at the point $z = 0$. We therefore replace the round-trip number p by the continuous variable t such as $E_p(t = pt_r, \xi) = E(t, \xi)$. We should then define the time derivative as $\partial E/\partial t = (E_{p+1} - E_p)/t_r$. Further approximations are needed, in particular, we assume that both linear ϕ and nonlinear cavity phase shift $L|E|^2$ are much smaller than unity. Furthermore, we assume that the length of the cavity is much shorter than the characteristic dispersion length of the fiber. Under these approximations, and by replacing $E_p(z = L)$ obtained from Eq. (3) in the cavity boundary condition expressed by Eq. (2), we get

$$t_r \frac{\partial E(t,\xi)}{\partial t} = TE_{in} + L\left(i\beta\frac{\partial^2 E(t,\xi)}{\partial \xi^2} + i|E(t,\xi)|^2 E(t,\xi)\right) + \left(1 - \frac{T^2}{2} - i\phi\right)E(t,\xi) + R'\exp(-i\phi')E(t-\tau,\xi). \quad (4)$$

The aim of this study is to analyze the impact of delay optical feedback on the spatiotemporal dynamics in the generic Lugiato–Lefever (LL) model.[1] We implement this optical feedback in the LLE by considering a single round-trip delay term.[38] This approximation to model the time-delayed feedback has been introduced in an early report modeled by Rosanov,[53] Lang and Kobayashi.[54] The LLE reads

$$\frac{\partial E}{\partial t} = i\beta\frac{\partial^2 E}{\partial \xi^2} - (1 + i\theta)E + i|E|^2 E + E_{in} + \eta e^{i\phi}E(t-\tau). \quad (5)$$

Here, $E(t, \xi)$ is the normalized amplitude of the electric field and θ is the frequency detuning between the injected light E_{in} and the cavity resonance. E_{in} is considered as being real without loss of generality. The feedback is characterized by the time-delayed τ, feedback strength η, and phase ϕ. Homogeneous steady state (HSSs) solutions E_S of Eq. (5) and their linear stability are analyzed in Ref. 38. Examples of the impact of the optical feedback on the shape of the $I_S(E_{in})$ curve and its stability are shown in Fig. 2.

III. LINEAR STABILITY ANALYSIS

The homogeneous steady state solutions of Eq. (5) satisfies

$$I_{in} = I_s\left[(1 - \eta\cos\phi)^2 + (I_s - \theta + \eta\sin\phi)^2\right], \quad (6)$$

where $I_{in} = E_{in}^2$ and $I_s = |E_s|^2$. The transmitted intensity as a function of the input intensity E_{in} is monostable if $\theta_{c-} < \theta < \theta_{c+}$, where $\theta_{c\pm} = \pm\sqrt{3} + \eta(\sin\phi \mp \sqrt{3}\cos\phi)$. If $0 < \theta < \theta_{c-}$ or $\theta > \theta_{c+}$, then the system exhibits a second-order critical point marking the onset of a hysteresis loop. For the case of no feedback ($\eta = 0$), the HSS are monostable ($\theta < \sqrt{3}$) or bistable ($\theta > \sqrt{3}$).[1] The coordinates of the critical point associated with bistability are strongly affected by the time-delayed feedback. The linear stability of the HSS with respect to finite frequency perturbations of the form $\exp(\sigma t + i\omega\xi)$ indicates that the homogeneous steady state can be destabilized by a modulational instability. Above the threshold associated with that instability there exists a finite band of Fourier modes $\omega_-^2 < \omega^2 < \omega_+^2$, with

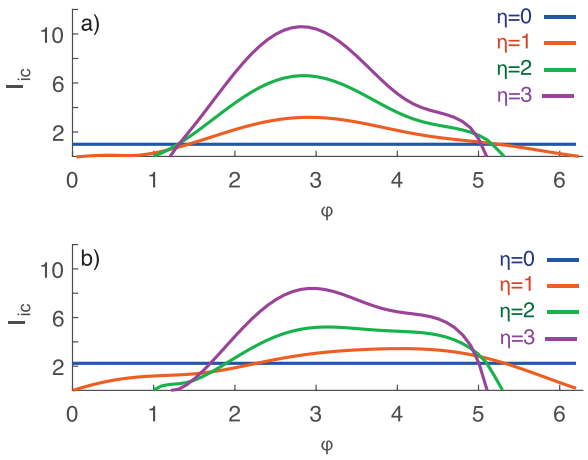

FIG. 2. The threshold E_{ic} as a function of the phase of the delay for different values of the strength of the delay [Eq. (10)]. (a) monostable case $\theta = 1$ and (b) bistable case $\theta = 3$.

$$\omega_\pm^2 = -\theta + 2I_s + \eta\sin\phi \pm \sqrt{I_s^2 - (1 - \eta\cos\phi)^2}, \quad (7)$$

which are linearly unstable and trigger the spontaneous evolution of the intra-cavity field towards a train of pulses that are stationary, spatially periodic, and occupy the whole space available in the double loop cavity. The threshold I_c and the critical frequency ω_c at the modulational instability are obtained when $\omega_-^2 = \omega_+^2$. The expressions are given by

$$I_c = 1 - \eta\cos\phi, \quad (8)$$

$$\omega_c = \sqrt{-\theta + \eta(\sin\phi - 2\cos\phi)}. \quad (9)$$

From the expression of I_c, we see that the threshold associated with the modulational instability is strongly impacted by the phase and the amplitude of the delay feedback. Indeed, for $-\pi/2 + k2\pi < \phi < \pi/2 + k2\pi$ with k is an integer number, the threshold is lowered $I_c < 1$. In terms of the injected intensity, the threshold reads

$$I_{ic} = E_{ic}^2 = [1 - \eta\cos\phi]\left[(1 - \eta\cos\phi)^2 + ((1 - \eta\cos\phi) - \theta + \eta\sin\phi)^2\right]. \quad (10)$$

The plot of the threshold associated with a modulational instability as a function of the phase of the feedback is presented in Fig. 2 for fixed values of the detuning parameter. From this figure, we can see that delayed feedback can control and either suppress the modulational instability or reduce the thresholds associated with this instability. The inclusion

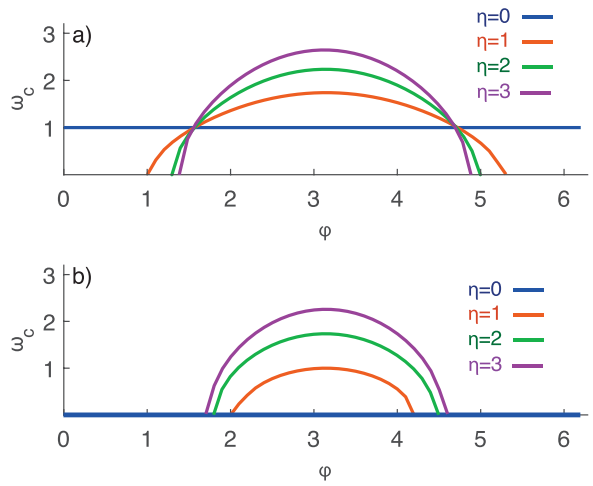

FIG. 3. The critical frequency ω_c as a function of the phase of the delay for different values of the strength of the delay [Eq. (9)]. (a) monostable case $\theta = 1$ and (b) bistable case $\theta = 3$.

of the feedback allows the modulational instability to have a finite domain of existence delimited by two phases of the delay as shown in Fig. 2. From a practical point of view, it is difficult to reach the high intensity regime in an experiment using a driven ring cavity made with an optical fiber operating with a continuous wave injected beam (CW operation). Most of the experiments used a synchronous pumping with a pulsed laser. Without delay feedback, the threshold is essentially determined by the detuning parameter. However, when considering an external all fiber loop, it is then possible to reduce drastically the threshold associated with the emergence of a periodic train of pulses. The most unstable critical frequency ω_c evaluated at the modulational instability threshold [Eq. (9)] provides the period of oscillation $T = 2\pi/\omega_c$ of solitons that emerge from the modulational instability. This critical frequency is plotted as a function of the phase of the feedback in Fig. 3 for a fixed detuning. We clearly see that the critical frequency is strongly impacted by the phase. By choosing an appropriate phase, the output field may have a very small period leading to the conception of all-optic systems for generation of signals with a high repetition rate. Finally, the marginal stability curves together with the characteristic input-intracavity field intensity are shown in Fig. 4.

IV. DRIFTING CAVITY SOLITONS AND ROGUE WAVES FORMATION

The LLE equation without delay feedback, i.e., $\eta = 0$, supports cavity solitons in a regime where the modulational instability appears subcritical, i.e., $\theta > 41/30$. The formation of a periodic train of pulses and cavity soliton formation are closely related. In the subcritical regime, there exists a hysteresis loop involving a homogeneous steady state and a periodic train of pulses. Within this hysteresis loop, there exists a pinning range of injected field intensities for which stable cavity solitons can be found even in the monostable case ($\theta < \sqrt{3}$).[55] They are similar to the localized structures and the localized patterns are found in relation with a generalized Swift–Hohenberg equation.[56] This theoretical prediction has been confirmed by experimental observation of cavity solitons in a cavity filled with liquid crystals[57] and in an all fiber cavity.[58] The interaction between CS's has been performed analytically and numerically by Vladimirov and collaborators in Ref. 59. The formation of CSs and their relation to optical comb generation in a standard silica fiber cavity[60,61] and in a continuous-wave driven nonlinear optical microresonators[62] has been recently established both numerically and experimentally. Optical frequency combs are sources with a spectrum consisting of millions of equally spaced laser lines. This unique property provides a link between the optical and the radiofrequency band of the electromagnetic spectrum and it has truly revolutionized a number of research disciplines, such as precision laser spectroscopy and frequency metrology. Experiments supported by numerical simulations of driven cavities such as whispering-gallery-mode microresonators leading to optical frequency comb generation have demonstrated the existence of complex spatiotemporal dynamics.[13] Similar complex dynamics have been observed in all fiber cavities.[63–66] Recently, it has been shown by using a rigorous tools of the dynamical system theory such as the Lyapunov exponent that this complex dynamics reported in literature belong to the spatiotemporal chaos type of behavior.[67]

In what follows, we focus on the effect of delayed feedback on the formation of cavity solitons. We fix the delay time and the phase, and we vary the strength of the feedback. In the course of time, we increase the strength of the delay as

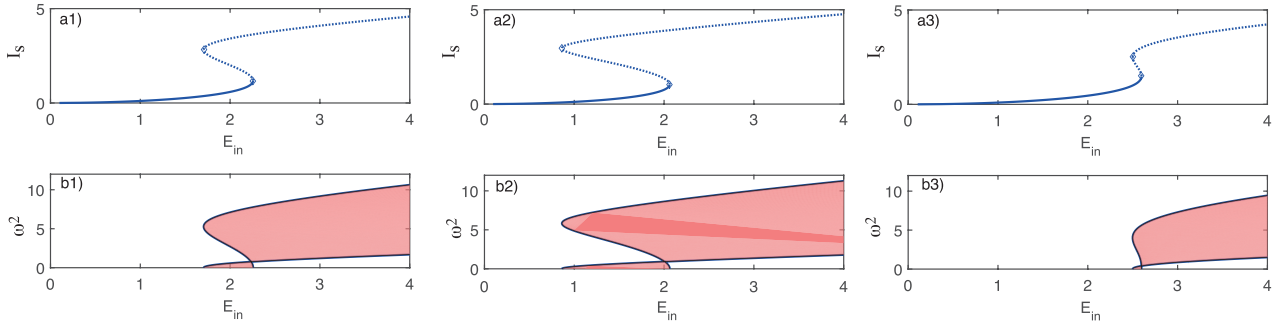

FIG. 4. The transmitted intensity as a function of the input intensity E_{in} for a fixed detuning parameter $\theta = 3$ but for different values on the time-delayed feedback parameters (a_1, a_2, and a_3) and marginal stability curves (b_1, b_2, and b_3) of the homogeneous solution of the Lugiato–Lefever model [Eq. (5)]. (a_1, b_1) without feedback $\eta = 0$ (a_2, b_2) feedback strength $\eta = 0.5$ and phase $\phi = 0$ (a_3, b_3) feedback strength $\eta = 0.5$ and phase $\phi = 0$. The stability marginal curves (b_1, b_2, and b_3) are obtained for zero eigenvalue ($\sigma = 0$). They correspond to the plot of Eq. (7) together with Eq. (6). The red color shading corresponds to modulationally unstable homogeneous steady states.

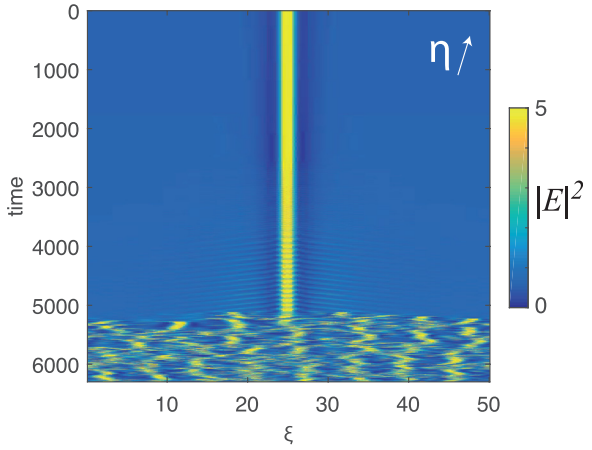

FIG. 5. ξ-time map showing the evolution of $|E|^2(\xi,t)$ in the LLE when increasing the feedback strength η from $\eta=0$ to $\eta=0.5$ with a step of 0.025 at each 300 time units. Cavity detuning is $\theta=3$, injection field is $E_{in}=2$, and feedback delay and phase are $\tau=10$ and $\phi=0$, respectively. The initial condition is the stationary cavity soliton.

shown in the τ-time map of Fig. 5. The first instability that appears is the self-pulsating cavity soliton. This behavior occurs even in the absence of delay feedback. However, a large intensity of the injected field is necessary to generate such self-pulsating CSs. Experimental evidence of self-pulsating structures has been provided for a synchronously pumped with a pulsed laser. The self-pulsating CS shown in Fig. 5 has been obtained for a moderate injected field. This indicates that the delay feedback renders the observation of self-pulsating CS possible even with the continuous wave regime with moderate injected power. Self-pulsating CSs emit radiation in the form of decaying dispersive waves which are asymmetric from both sides of CS. The asymmetry of radiation emission is due to the time-delayed feedback. When further increasing the strength of the delayed feedback, a transition towards a complex behavior as shown in Fig. 5 takes place. This figure has been obtained by using an initial condition that consists of stationary CSs. If we start numerical simulations with a periodic train of pulses and increase the time-delayed feedback, the dynamics leads to

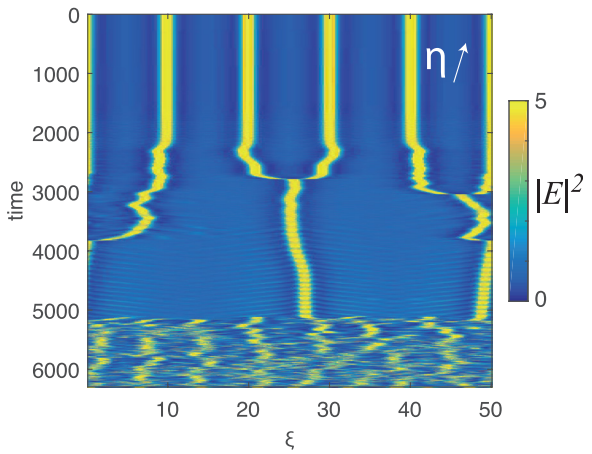

FIG. 6. ξ-time map showing the evolution of $|E|^2(\xi,t)$ in the LLE when increasing the feedback strength η from $\eta=0$ to $\eta=0.5$ with a step of 0.025 at each 300 time units. The parameters are the same as for Fig. 7 except for the initial condition which is a stationary periodic structure.

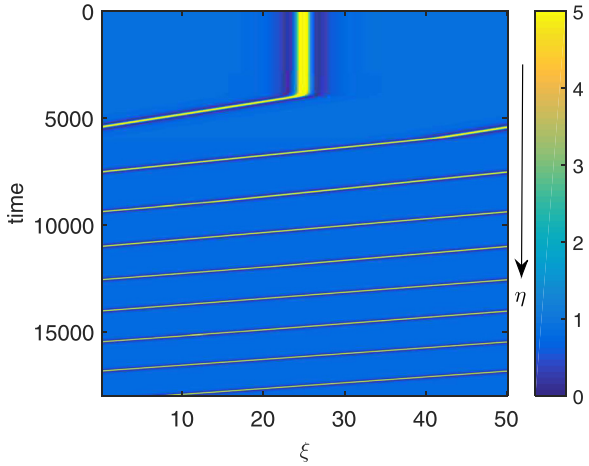

FIG. 7. ξ-time maps showing the evolution of $|E|^2(\xi,t)$ in the LLE when increasing the feedback strength η from $\eta=0$ to $\eta=0.1$ with a step of 0.02 at each 3000 time units. Cavity detuning is $\theta=3$, injection field is $E_{in}=2.2$, and feedback delay and phase are $\tau=100$ and $\phi=\pi$, respectively. The initial condition is the stationary cavity soliton.

the same complex spatiotemporal regime as shown in numerical simulations of the model Eq. (5) (see Fig. 6). Before reaching this regime, we can see a drifting and self-pulsating CSs.

With increasing the injected field intensity, the τ-time map shows a drift of CS—see Fig. 7. This phenomenon has been reported in.[38] The drift instability is attributed to the time-delayed feedback. It is well know that the CS exhibits radiation due to the dispersive waves from a localized state of two counter-propagative fronts. In the absence of delay, the CS radiates symmetrically from both sides (right and left). However, when considering the delay feedback, the τ-time maps obtained from a fixed value of the strength of the delay, show clearly an asymmetric emission of dispersive waves as visible in Fig. 8. The critical point associated with the traveling wave coincides with the threshold associated with the drift instability. This threshold depends on the phase of the delayed feedback. For instance, for $\phi=\pi$, the threshold is $\tau\eta=1$.

In the rest of this paper, we focus the analysis on the formation of rogue waves in the LLE with time delayed

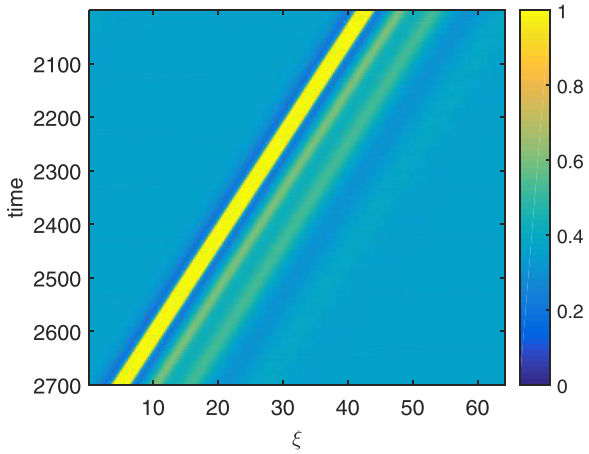

FIG. 8. Drifting CS with an asymmetric radiation of dispersive waves for $\eta=0.9$ and $\phi=5\pi/4$. Other parameters are the same as in the figure.

feedback. They consist of rare giant short optical pulses propagating in the cavity. The experimental observation of optical rogue waves has been identified in the context of nonlinear fiber optics as large peaks appearing in the supercontinuum generated by a photonic crystal fiber.[46] The modulational instability mechanism together with pulse collisions has been discussed in an earlier report by Peregrine.[68] Experimental confirmation of the collision based mechanism for rogue wave formation, has been demonstrated in optical fibers[69,70] and in water-wave-tank[71,72] systems. In the framework of the nonlinear Schrödinger equation, an analytical study of the nonlinear interaction between two frequency solitons in the form of Akhmediev breathers has been reported in Ref. 73. The nonlinear Schrödinger equation is one of the fundamental equations in nonlinear physics that describes conservative waves. For instance, this equation has been largely used as a prototype for the study of rogue waves in fluid mechanics and in nonlinear fiber optics. However, the nonlinear Schrödinger equation is not an adequate model to describe nonlinear resonators because it does not include dissipation and pumping. The LLE model is more appropriate for this purpose because it admits dissipative rogue waves like solitons. This concept has been introduced by Akhmediev in one-dimensional passively mode-locked laser systems.[74] In dissipative homogeneous systems such as small area semiconductor devices where dispersion and diffraction are negligible, numerical simulation supported by experimental results indicate the possibility of formation of rogue waves.[75] It has also been shown that when a delay feedback is taken into account extreme events are generated.[45] Rogue waves formation resides in the fact the system exhibits a sudden appearance or disappearance of a strange attractor, this mechanism is called as crisis in the dynamical system theory. This bifurcation occurs when a chaotic attractor is close to a set of unstable periodic orbits or its stable manifold. In spatially extended systems such as a broad areas laser with saturable absorber, it has been predicted theoretically and proved experimentally that the emergence of spatiotemporal chaos leads to the formation of rogue waves.[51,52] This mechanism corresponds to an alternation of regular and irregular dynamics in the course of time evolution. However, depending on the level of the pumping current, the system can exhibit a route to spatiotemporal chaos *via* quasi-periodicity (torus bifurcation).[52,76] A similar experimental result has been observed in a liquid crystal light valve with optical feedback.[77] The collision mechanism leading to the formation of dissipative rogue waves has been establish numerically in the Lugiato–Lefever model without delay feedback.[14]

Random formation of coherent structures having properties of localization in space and time similar to rogue waves has been proposed in relation with integrable turbulence.[78] Defining a rogue wave is still an open issue. Recently, it has been proposed as an optical pulse whose amplitude or intensity is much higher than that of the surrounding pulses. The main characteristic of the rogue wave formation is their pulse height probability distribution: if it possesses a long tail, then we can qualify this behavior as an evidence for rogue wave formation. We compute the number of events as a function of the intensity of the pulses in a semi-logarithmic scale. The

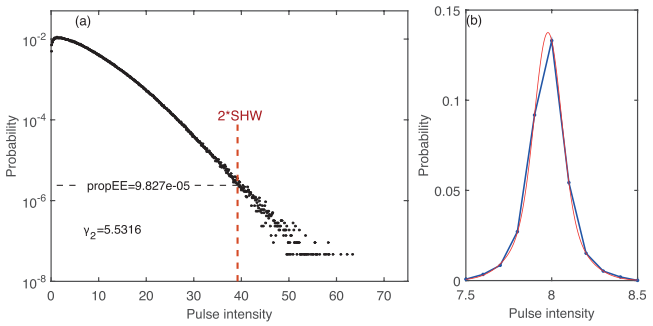

FIG. 9. (a) Probability density function (black dots) of the intensity of the pulses in the semi-logarithmic scale. The dashed line indicates 2 times the significant wave height (SWH). The LLE parameters are $\theta = 3$ and $E_{in} = 2.2$ and the feedback parameters are $\tau = 100$, $\eta = 0.9$ and $\phi = 0$. (b) Probability density function (blue line and dots) of the intensity of the pulses for a week feedback with a strength of $\eta = 0.05$. The red solid line shows Gaussian fit to the data.

results are shown Fig. 9. When the feedback strength is small, the pulse height probability distribution is rather Gaussian as indicated by the red color in Fig. 9(b). When we increase the feedback strength Fig. 9(b) the pulse height probability distribution evolves towards an L-shape distribution with a long tail–see Fig. 9(b). We have estimated the proportion of extreme events PEE and the excess kurtosis γ_2. The values are indicated in Fig. 9(a). These values suggest that the statistics of rogue wave are far from gaussian distribution. These results are obtained from numerical simulations of the LLE with delay feedback with periodic boundary conditions. An example of the rogue wave formation is shown in the τ-time map presenting the evolution of $|E|^2(\tau, t)$ for a moderate intensity of the injected field (cf. Fig. 10). The modulational instability mechanism together with pulse collisions is considered in the literature as the main mechanism for the generation of rogue waves. This is clearly visible in the ξ-time map of Fig. 10. The collision process between pulses is enhanced by the delay feedback. More recently, two-dimensional dissipative rogue waves have been reported in the framework of the LLE[79] and in the laser with saturable absorber with delay feedback.[80,81] In this

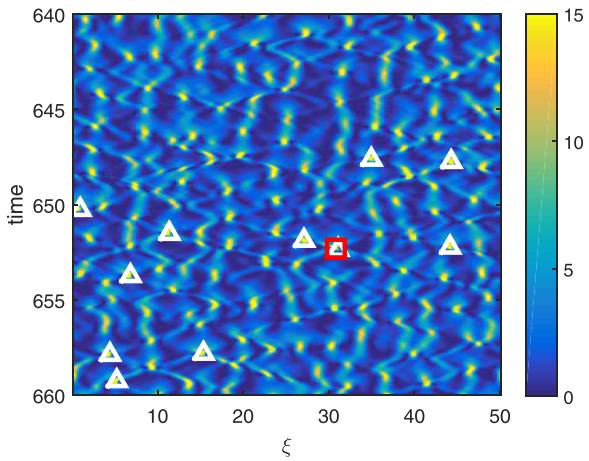

FIG. 10. Space-time evolution of $|E|^2(\xi, t)$ for fixed LLE parameters of $\theta = 3$ and $E_{in} = 2.2$ and feedback parameters $\tau = 100$, $\eta = 0.9$ and $\phi = 0$. Events with amplitude $P(\xi) = |E|^2(\xi, t) > 35$ are shown with (white) triangles and with $P(\xi) = |E|^2(\xi, t) > 45$ with (red) square.

context, transition from stationary to chaotic two-dimensional cavity solitons through the period doubling route has been reported.[82]

V. CONCLUSIONS

We have investigated the formation of temporal cavity solitons, self-pulsating cavity solitons, and rogue wave generation in a standard silica fiber cavity or microresonator. Both systems are well described by the paradigmatic Lugiato–Lefever equation. We have analyzed the effect of time-delayed feedback control of the dynamics of these nonlinear objects. In the spatial cavities, the time-delayed feedback has been incorporated to control both drifting cavity solitons and rogue wave formation in one and in two dimensional settings. In this paper, we have analyzed a temporal analog of the spatial cavities with a delay feedback leading to the optical frequency comb generation, namely driven cavities such as whispering-gallery-mode microresonators and all fiber cavities. We have shown that the delay feedback can induce the drift of temporal cavity solitons. In the absence of time-delayed feedback control, temporal cavity solitons do not drift. We have shown also that radiation emitted from drifting cavity solitons is asymmetric. This broken symmetry is clearly attributed to the time-delayed feedback. Finally, we have shown that a rogue wave regime can be reached for a moderate injected field intensities. This opens a possibility of experimental observation of temporal dissipative rogue waves in continuous-wave driven nonlinear optical microresonators.

Note added in proof. After submission of this paper, we realized that the work by Julien Javaloyes describes a similar pattern evolution in a cavity composed of a gain medium coupled to a saturable absorber.[83] We consider that this paper is relevant for our contribution.

ACKNOWLEDGMENTS

M.T. received support from the Fonds National de la Recherche Scientifique (Belgium). M.G.C. and M.T. acknowledge the support of the CONICYT Project No. REDES-150046. We acknowledge the support of the Interuniversity Attraction Poles program Photonics@be of the Belgian Science Policy Office (BelSPO), under Grant No. IAP 7-35. K.P. is grateful to the Methusalem foundation for financial support.

[1]L. A. Lugiato and R. Lefever, Phys. Rev. Lett. **58**, 2209 (1987).
[2]A. M. Turing, Philos. Trans. R. Soc. London B: Biol. Sci. **237**, 37 (1952).
[3]I. Prigogine and R. Lefever, J. Chem. Phys. **48**, 1695 (1968).
[4]P. Glansdorff and I. Prigogine, *Thermodynamic Theory of Structure, Stability and Fluctuations* (Wiley Interscience, 1971).
[5]V. Odent, M. Tlidi, M. G. Clerc, P. Glorieux, and E. Louvergneaux, Phys. Rev. A **90**, 011806 (2014).
[6]P. Kockaert, P. Tassin, G. Van der Sande, I. Veretennicoff, and M. Tlidi, Phys. Rev. A **74**, 033822 (2006).
[7]L. Gelens, G. Van der Sande, P. Tassin, M. Tlidi, P. Kockaert, D. Gomila, I. Veretennicoff, and J. Danckaert, Phys. Rev. A **75**, 063812 (2007).
[8]U. Peschel, O. Egorov, and F. Lederer, Opt. Lett. **29**, 1909 (2004).
[9]M. Haelterman, S. Trillo, and S. Wabnitz, Opt. Commun. **91**, 401 (1992).
[10]Y. K. Chembo and C. R. Menyuk, Phys. Rev. A **87**, 053852 (2013).
[11]T. Hansson, D. Modotto, and S. Wabnitz, Phys. Rev. A **88**, 023819 (2013).
[12]Y. K. Chembo and N. Yu, Phys. Rev. A **82**, 033801 (2010).
[13]Y. K. Chembo, D. V. Strekalov, and N. Yu, Phys. Rev. Lett. **104**, 103902 (2010).
[14]A. Coillet, J. Dudley, G. Genty, L. Larger, and Y. K. Chembo, Phys. Rev. A **89**, 013835 (2014).
[15]A. Coillet and Y. K. Chembo, Chaos **24**, 013113 (2014).
[16]M. Tlidi, M. Haelterman, and P. Mandel, Europhys. Lett. **42**, 505 (1998).
[17]M. Tlidi, M. Haelterman, and P. Mandel, Quantum Semiclassical Opt. **10**, 869 (1998).
[18]M. Tlidi, J. Opt. B: Quantum Semiclassical Optics **2**, 438 (2000).
[19]N. Veretenov and M. Tlidi, Phys. Rev. A **80**, 023822 (2009).
[20]M. Tlidi, M. Taki, and T. Kolokolnikov, Chaos **17**, 037101 (2007).
[21]*Dissipative Solitons: From Optics to Biology and Medicine*, Lecture Notes in Physics, edited by N. Akhmediev and A. Ankiewicz, Vol. 751 (Springer, Heidelberg, 2008).
[22]O. Descalzi, M. G. Clerc, S. Residori, and G. Assanto, *Localized States in Physics: Solitons and Patterns: Solitons and Patterns* (Springer, 2011).
[23]H. Leblond and D. Mihalache, Phys. Rep. **523**, 61 (2013).
[24]D. Mihalache, Rom. Rep. Phys. **67**, 1383 (2015).
[25]Y. He, X. Zhu, and D. Mihalache, Rom. J. Phys. **61**, 595 (2016).
[26]D. Mihalache, Rom. Rep. Phys. **69**, 403 (2017).
[27]M. Tlidi, K. Staliunas, K. Panajotov, A. G. Vladimiorv, and M. Clerc, Philos. Trans. R. Soc. A **372**, 20140101 (2014).
[28]L. Lugiato, F. Prati, and M. Brambilla, *Nonlinear Optical Systems* (Cambridge University Press, 2015).
[29]*Nonlinear Dynamics: Materials, Theory and Experiments*, edited by M. Tlidi and M. G. Clerc (Springer Proceedings in Physics, 2016), Vol. 173.
[30]E. Thomas, *Applied Delay Differential Equations* (Springer, 2009).
[31]M. Tlidi, A. G. Vladimirov, D. Pieroux, and D. Turaev, Phys. Rev. Lett. **103**, 103904 (2009).
[32]S. V. Gurevich and R. Friedrich, Phys. Rev. Lett. **110**, 014101 (2013).
[33]M. Tlidi, A. G. Vladimirov, D. Turaev, G. Kozyreff, D. Pieroux, and T. Erneux, Eur. Phys. J. D **59**, 59 (2010).
[34]K. Panajotov and M. Tlidi, Eur. Phys. J. D **59**, 67 (2010).
[35]M. Tlidi, E. Averlant, A. G. Vladimirov, and K. Panajotov, Phys. Rev. A **86**, 033822 (2012).
[36]A. Pimenov, A. G. Vladimirov, S. V. Gurevich, K. Panajotov, G. Huyet, and M. Tlidi, Phys. Rev. A **88**, 053830 (2013).
[37]A. G. Vladimirov, A. Pimenov, S. V. Gurevich, K. Panajotov, E. Averlant, and M. Tlidi, Philos. Trans. R. Soc. A **372**, 20140013 (2014).
[38]K. Panajotov, D. Puzyrev, A. G. Vladimirov, S. V. Gurevich, and M. Tlidi, Phys. Rev. A **93**, 043835 (2016).
[39]T. Erneux, G. Kozyreff, and M. Tlidi, Philos. Trans. R. Soc. A **368**, 483 (2010).
[40]M. Tlidi, A. Sonnino, and G. Sonnino, Phys. Rev. E **87**, 042918 (2013).
[41]S. V. Gurevich, Phys. Rev. E **87**, 052922 (2013).
[42]S. V. Gurevich, Philos. Trans. R. Soc. A **372**, 20140014 (2014).
[43]M. Tlidi, Y. Gandica, G. Sonnino, E. Averlant, and K. Panajotov, Entropy **18**, 64 (2016).
[44]D. Puzyrev, S. Yanchuk, A. G. Vladimirov, and S. V. Gurevich, SIAM J. Appl. Dyn. Syst. **13**, 986 (2014).
[45]J. A. Reinoso, J. Zamora-Munt, and C. Masoller, Phys. Rev. E **87**, 062913 (2013).
[46]D. R. Solli, C. Koonath, and B. Jalali, "Optical Rogue waves," Nature **450**, 1054 (2007).
[47]N. Akhmediev, J. M. Dudley, D. R. Solli, and S. K. Turitsyn, J. Opt. **15**, 060201 (2013).
[48]M. Onorato, S. Residori, U. Bortolozzo, A. Montina, and F. T. Arecchi, Phys. Rep. **528**, 47 (2013).
[49]M. Dudley, F. Dias, M. Erkintalo, and G. Genty, Nat. Photonics **8**, 755 (2014).
[50]N. Akhmediev, B. Kibler, F. Baronio, M. Belic, W. P. Zhong, Y. Zhang, W. Chang, J. M. Soto-Crespo, P. Vouzas, P. Grelu, C. Lecaplain, K. Hammani, S. Rica, A. Picozzi, M. Tlidi, K. Panajotov, A. Mussot, A. Bendahmane, P. Szriftgiser, G. Genty, J. Dudley, A. Kudlinski, A. Demircan, U. Morgner, S. Amiraranashvili, C. Bree, G. Steinmeyer, C. Masoller, N. G. R. Broderick, A. F. J. Runge, M. Erkintalo, S. Residori, U. Bortolozzo, F. T. Arecchi, S. Wabnitz, C. G. Tiofack, S. Coulibaly, and M. Taki, J. Opt. **18**, 063001 (2016).
[51]F. Selmi, S. Coulibaly, Z. Loghmari, I. Sagnes, G. Beaudoin, M. G. Clerc, and S. Barbay, Phys. Rev. Lett. **116**, 013901 (2016).
[52]S. Coulibaly, M. G. Clerc, F. Selmi, and S. Barbay, Phys. Rev. A **95**, 023816 (2017).
[53]N. N. Rosanov, Sov. J. Quantum Electron. **4**(10), 1191 (1975).
[54]R. Lang and K. Kobayashi, IEEE Quantum Electron. **16**, 347 (1980).

[55]A. J. Scroggie, W. J. Firth, G. S. McDonald, M. Tlidi, R. Lefever, and L. A. Lugiato, Chaos, Solitons Fractals **4**, 1323 (1994).
[56]M. Tlidi, P. Mandel, and R. Lefever, Phys. Rev. Lett. **73**, 640 (1994).
[57]V. Odent, M. Taki, and E. Louvergneaux, New J. Phys. **13**, 113026 (2011).
[58]F. Leo, S. Coen, P. Kockaert, S.-P. Gorza, P. Emplit, and M. Haelterman, Nat. Photonics **4**, 471 (2010).
[59]D. Turaev, A. G. Vladimirov, and S. Zelik, Phys. Rev. Lett. **108**, 263906 (2012).
[60]S. Coen, H. G. Randle, T. Sylvestre, and M. Erkintalo, Opt. Lett. **38**, 37 (2013).
[61]S. Coen and M. Erkintalo, Opt. Lett. **38**, 1790 (2013).
[62]T. Herr, V. Brasch, J. D. Jost, C. Y. Wang, N. M. Kondratiev, M. L. Gorodetsky, and T. J. Kippenberg, Nat. Photonics **8**, 145 (2014).
[63]F. Mitschke, G. Steinmeyer, and A. Schwache, Physica D **96**, 251 (1996).
[64]G. Steinmeyer, A. Schwache, and F. Mitschke, Phys. Rev. E **53**, 5399 (1996).
[65]F. Leo, L. Gelens, P. Emplit, M. Haelterman, and S. Coen, Opt. Express **21**, 9180 (2013).
[66]M. Anderson, F. Leo, S. Coen, M. Erkintalo, and S. G. Murdoch, Optica **3**, 1071 (2016).
[67]Z. Liu, M. Ouali, S. Coulibaly, M. G. Clerc, M. Taki, and M. Tlidi, Opt. Lett. **42**, 1063 (2017).
[68]D. H. Peregrine, J. Aust. Math. Soc., Ser. B **25**, 16 (1983).
[69]A. Mussot, E. Louvergneaux, N. Akhmediev, F. Reynaud, L. Delage, and M. Taki, Phys. Rev. Lett. **101**, 113904 (2008).
[70]B. Kibler, J. Fatome, C. Finot, G. Millot, F. Dias, G. Genty, N. Akhmediev, and J. M. Dudley, Nat. Phys. **6**, 790 (2010).
[71]A. Chabchoub, N. P. Hoffmann, and N. Akhmediev, Phys. Rev. Lett. **106**, 204502 (2011).
[72]A. Chabchoub, N. Akhmediev, and N. P. Hoffmann, Phys. Rev. E **86**, 016311 (2012).
[73]N. Akhmediev, J. M. Soto-Crespo, and A. Ankiewicz, Phys. Lett. A **373**, 2137 (2009).
[74]J. M. Soto-Crespo, P. Grelu, and N. Akhmediev, Phys. Rev. E **84**, 016604 (2011).
[75]C. Bonatto, M. Feyereisen, S. Barland, M. Giudici, C. Masoller, J. R. Leite, J. R. Tredicce, C. Bonatto, M. Feyereisen, S. Barland, M. Giudici, and C. Masoller, Phys. Rev. Lett **107**, 053901 (2011).
[76]K. Panajotov, M. G. Clerc, and M. Tlidi, Eur. Phys. J. D **71**, 176 (2017).
[77]M. G. Clerc, G. González-Cortés, and M. Wilson, Opt. Lett. **41**, 2711 (2016).
[78]P. Suret, R. El Koussaifi, A. Tikan, C. Evain, S. Randoux, C. Szwaj, and S. Bielawski, Nat. Commun. **7**, 13136 (2016).
[79]M. Tlidi and K. Panajotov, Chaos **27**, 013119 (2017).
[80]C. Rimoldi, S. Barland, F. Prati, and G. Tissoni, J. Nonlinear Phenom. Complex Syst. **20**, 73 (2017).
[81]C. Rimoldi, S. Barland, F. Prati, and G. Tissoni, Phys. Rev. A **95**, 023841 (2017).
[82]K. Panajotov and M. Tlidi, Opt. Lett. **39**, 4739 (2014).
[83]J. Javaloyes, Phys. Rev. Lett. **116**, 043901 (2016).